

Supplementary Information

Regulatory effect of triphenylphosphine oxide on perovskites for morphological and radiative improvement

Danyang Jiang,^a Tao Jiang,^b Yuee Tian,^a Kaichuan Wen,^b Chunbo Duan,^a Nana
Wang,^{*b} Qiang Li,^{*a} Jianpu Wang,^{*b} and Hui Xu^{*a}

^aKey Laboratory of Functional Inorganic Material Chemistry (Chinese Ministry of Education), Heilongjiang University, 74 Xuefu Road, Harbin 150080, China.

^bKey Laboratory of Flexible Electronics (KLOFE) & Institute of Advanced Materials (IAM), Jiangsu National Synergetic Innovation Center for Advanced Materials (SICAM), Nanjing Tech University (NanjingTech), 30 South Puzhu Road, 211816 Nanjing, China.

Experimental Section

Materials. High-purity (99.99%) PbBr_2 was purchased from TCI. FABr with a purity of more than 99.5% were purchased from Maituowei. All the materials were used without further purification. FAPbBr_3 solution was formulated by dissolving FABr and PbBr_2 powders in dimethyl sulfoxide (DMSO) at a molar ratio of 2:1, with 0.30 M concentration of FAPbBr_3 in DMSO. The molar ratio of TPPO and FAPbBr_3 is 0.01, 0.02, 0.03, 0.04, 0.05, 0.06 and 0.07:1. After this, all solutions were stirred overnight at the rate of 4000 rpm.

Film preparation. ITO glass substrates were sequentially cleaned by acetone, ultrasonication with diluted detergent, deionized water and ethanol each for 20 min. The ITO/glass substrates were dried under pure N_2 gas stream and exposed to UV-ozone plasma for 15 min prior to film samples fabrication. FAPbBr_3 emission layer was deposited on the ITO/glass substrates by spin-coating at a rotation speed of 4000 rpm for 50 s using the different ratio of $x\%$ TPPO: FAPbBr_3 mixture solutions, followed by annealing at 80°C for 10 min in a N_2 -purged glove-box, with O_2 and H_2O levels 0.5 ppm. The film thickness was measured with Bruker Dektak150, with an average value of ~ 400 nm.

Sample Characterization. SEM images were obtained using a Hitachi S-4800 field emission scanning electron microscope. X-ray photoelectron spectroscopy (XPS) analysis was performed on a VG ESCALAB MK II with an Mg Ka (1253.6 eV) achromatic X-ray source. Photoluminescence (PL) emission spectra of the target compound was measured using a SHIMADZU UV-3150 spectrophotometer and a SHIMADZU RF-5301PC spectrophotometer, respectively. Photoluminescence quantum yields (PLQY, η_{PL}) of these films were measured through a labsphere 1-M-2 ($\phi = 6''$) integrating sphere coated by Benflect with efficient light reflection in a wide range of 200-1600 nm, which was integrated with FPLS 1000. The absolute η_{PL} determination of the sample was performed by two spectral (emission) scans, with the emission monochromator scanning over the Rayleigh scattered light from the sample and from a blank substrate. The first spectrum recorded the scattered light and the

emission of the sample, and the second spectrum contained the scattered light of Benflect coating. The integration and subtraction of the scattered light parts in these two spectra arrived at the photon number absorbed by the samples (N_a); while, integration of the emission of the samples to calculate the emissive photon number (N_e). Then, the absolute n_{PL} can be estimated according to the equation of $\eta_{PL} = N_e/N_a$. Spectral correction (emission arm) was applied to the raw data after background subtraction, and from these spectrally corrected curves the quantum yield was calculated using aF900 software wizard.

Device Fabrication: Patterned ITO glass substrates were sequentially cleaned with acetone, detergent, deionized water and ethanol in a sonic bath for 15 minutes, then use a nitrogen gun to blow dry. Prior to device fabrication, the substrates were treated by oxygen plasma for 15 min. The HIL was prepared by spin coating PEDOT:PSS (4083) at 3000 rpm for 50s onto the ITO substrate followed by baking at 120 °C for 20 min in air forming a 40 nm-thick film. Subsequently, the substrates are transferred into a nitrogen glove box (H_2O and $O_2 \leq 0.5$ ppm). And FAPbBr₃ perovskite film was spin coated at 3500 rpm for 50s and annealed at 65 °C for 12 min. After thermal annealing, the samples are transferred into a vacuum chamber. The layers of DPEPO (10nm), DBTDPO (45nm), LiF (1nm) and Al (100nm) were subsequently thermally evaporated under the vacuum of 4×10^{-5} Pa through a shadow mask to produce active area of 0.04 cm².

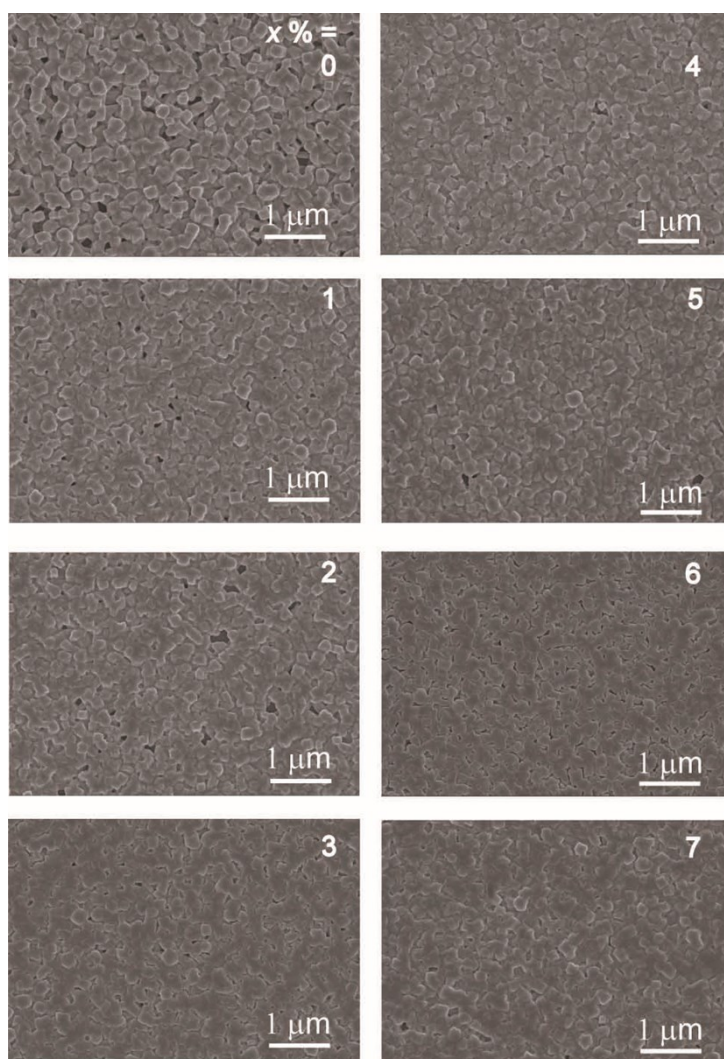


Fig. S1. SEM images of $x\%$ TPPO:FAPbBr₃ films. Numbers showed in images are x .

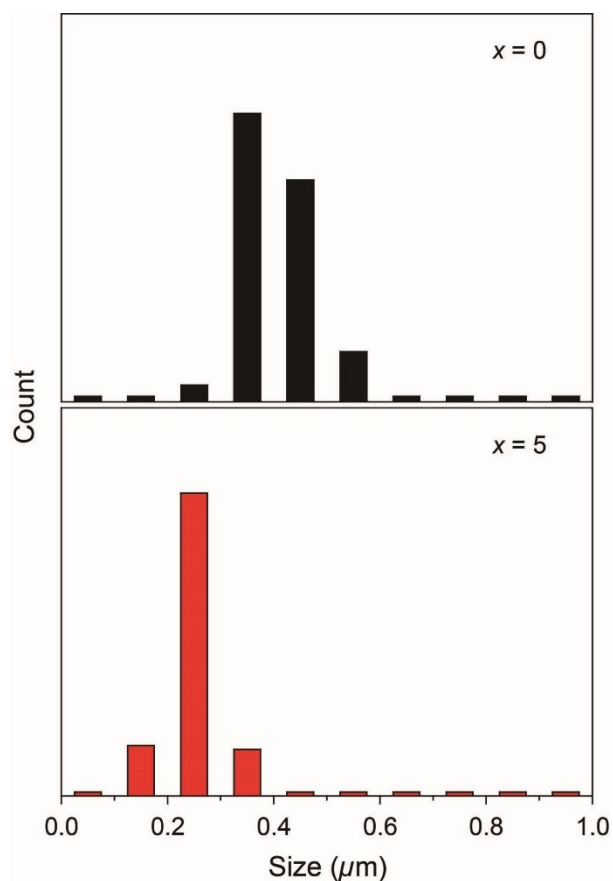


Fig. S2. Comparison on statistical grain size distributions of $x\%$ TPPO:FAPbBr₃ films ($x = 0$ and 5).

Crystal sizes of pure FAPbBr₃ perovskite film were between 0.3-0.6 μm, corresponding to an average crystal size of 0.4 μm. However, adding 5% TPPO markedly reduced crystal sizes of the film to 0.2-0.3 μm and simultaneously improved size uniformity, corresponding to an average crystal size of 0.25 μm.

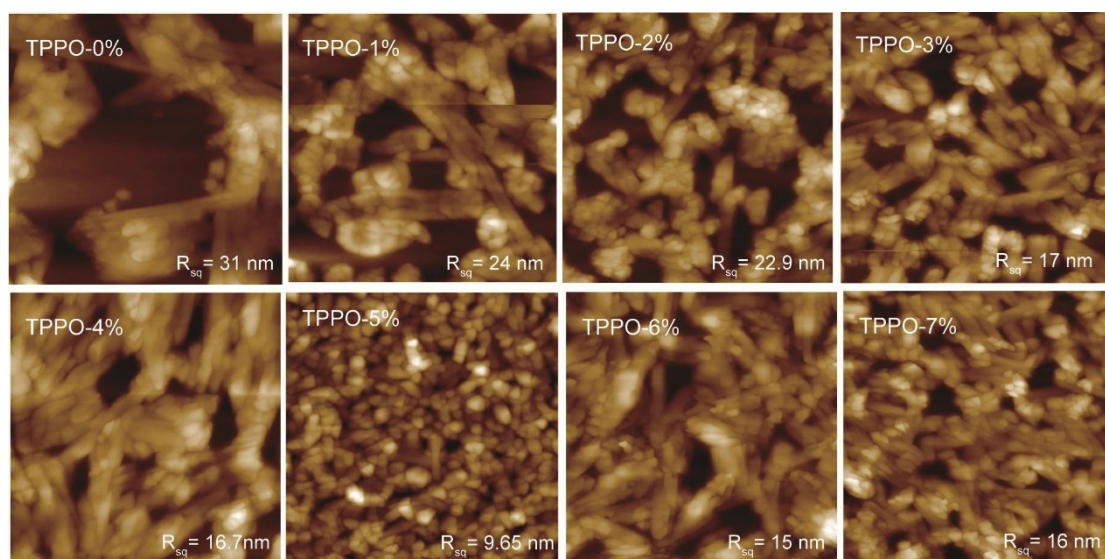


Fig. S3. Atom force microscopy images of $x\%$ TPPO:FAPbBr₃ films ($x = 0-7$).

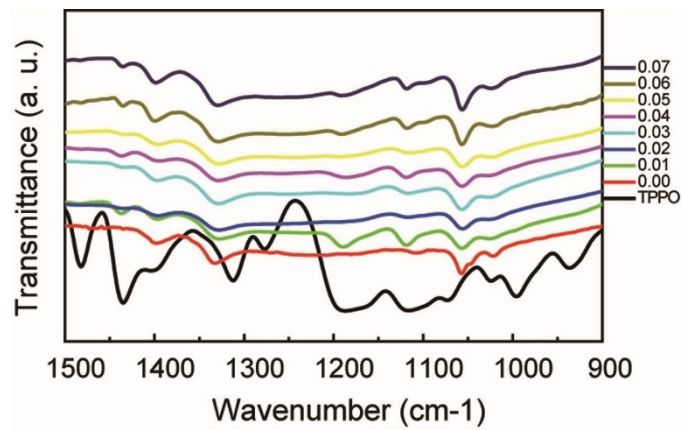


Fig. S4. Fourier transformed infrared (FTIR) spectra of TPPO and $x\%$ TPPO:FAPbBr₃. The powders of the films were obtained through scraping off substrates.

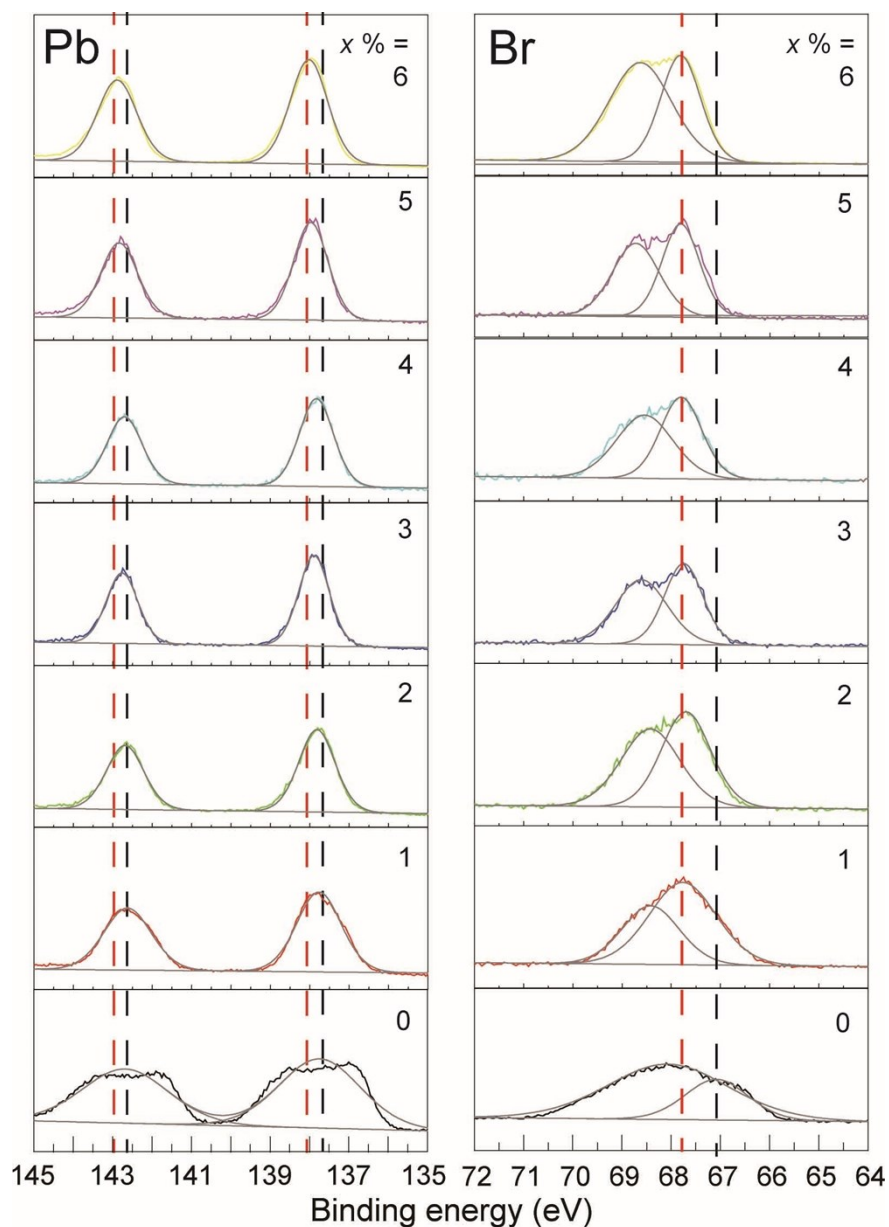


Fig. S5. XPS measurements of $x\%$ TPPO:FAPbBr₃ perovskite films regarding to the elements specific areas for Pb 4f and Br 3d with the corresponding peak fitting. The black dash lines indicate the peak positions of neat FAPbBr₃ film, while the red dash lines show the peak shifts after $x\%$ TPPO addition.

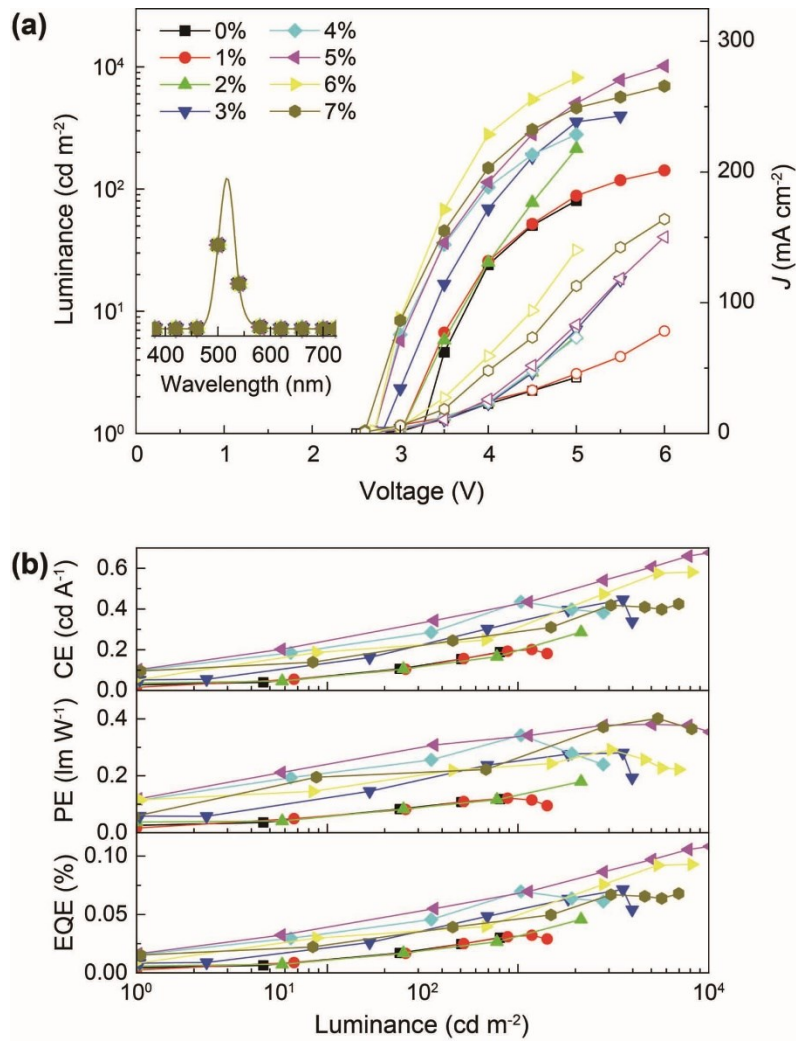


Fig. S6. (a) Luminance-Voltage-Current density (J) characteristics of PeLEDs; (b) Efficiency-Luminance relationships.

Perovskite light-emitting diodes (PeLED) based on structure of ITO|PEDOT:PSS (40 nm)| $x\%$ TPPO:FAPbBr₃ (45 nm)|DPEPO (10 nm)|DBTDPO (45 nm)|LiF (1 nm)|Al (100 nm) were fabricated, in which PEDOT:PSS and DBTDPO are poly(3,4-ethylenedioxythiophene):poly(styrenesulfonate) and 4,6-bis(diphenylphosphoryl)dibenzothiophene, used as hole and electron transporting layers, respectively, and DPEPO is bis[2-(diphenylphosphino)phenyl]ether oxide as hole blocking layer. It is showed that the maximum luminance of the devices was firstly increased from 80 cd m⁻² at $x = 0$ to ~ 1000 cd m⁻² at $x = 5$, and then decreased to ~ 700 cd m⁻² at $x = 7$. Furthermore, the efficiencies of the devices were consistent to η_{PL} values of the corresponding emissive layers.

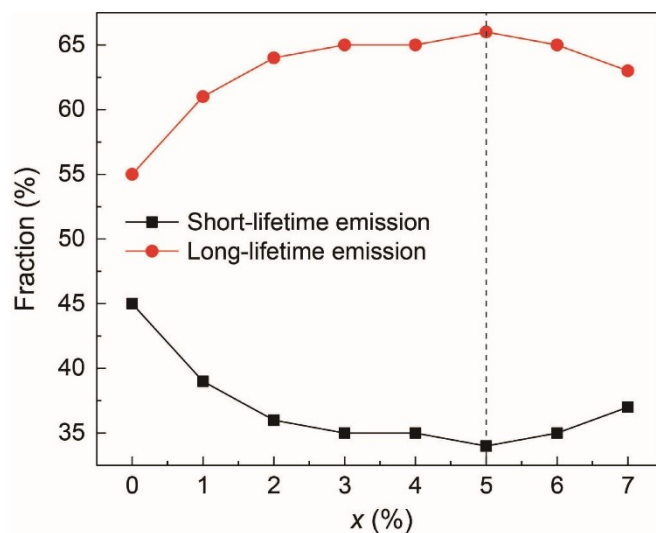


Fig. S7. Fraction variation of short and long-lifetime components for $x\%$ TPPO:FAPbBr₃ films ($x = 0-7$).

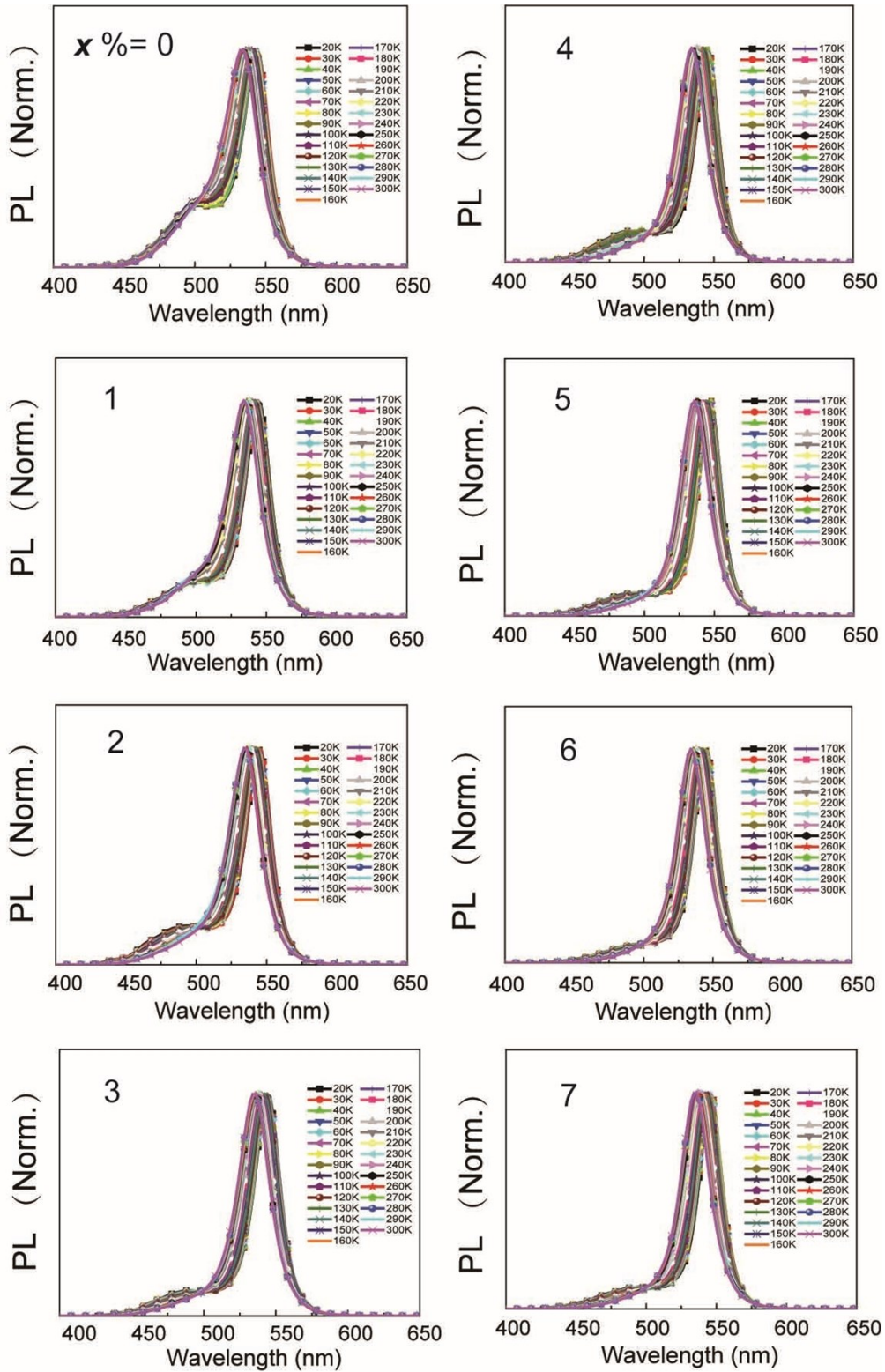


Fig. S8. PL spectra of $x\%$ TPPO:FAPbBr₃ films ($x = 0-7$) at temperature range of 20-300 K with an interval of 10 K.

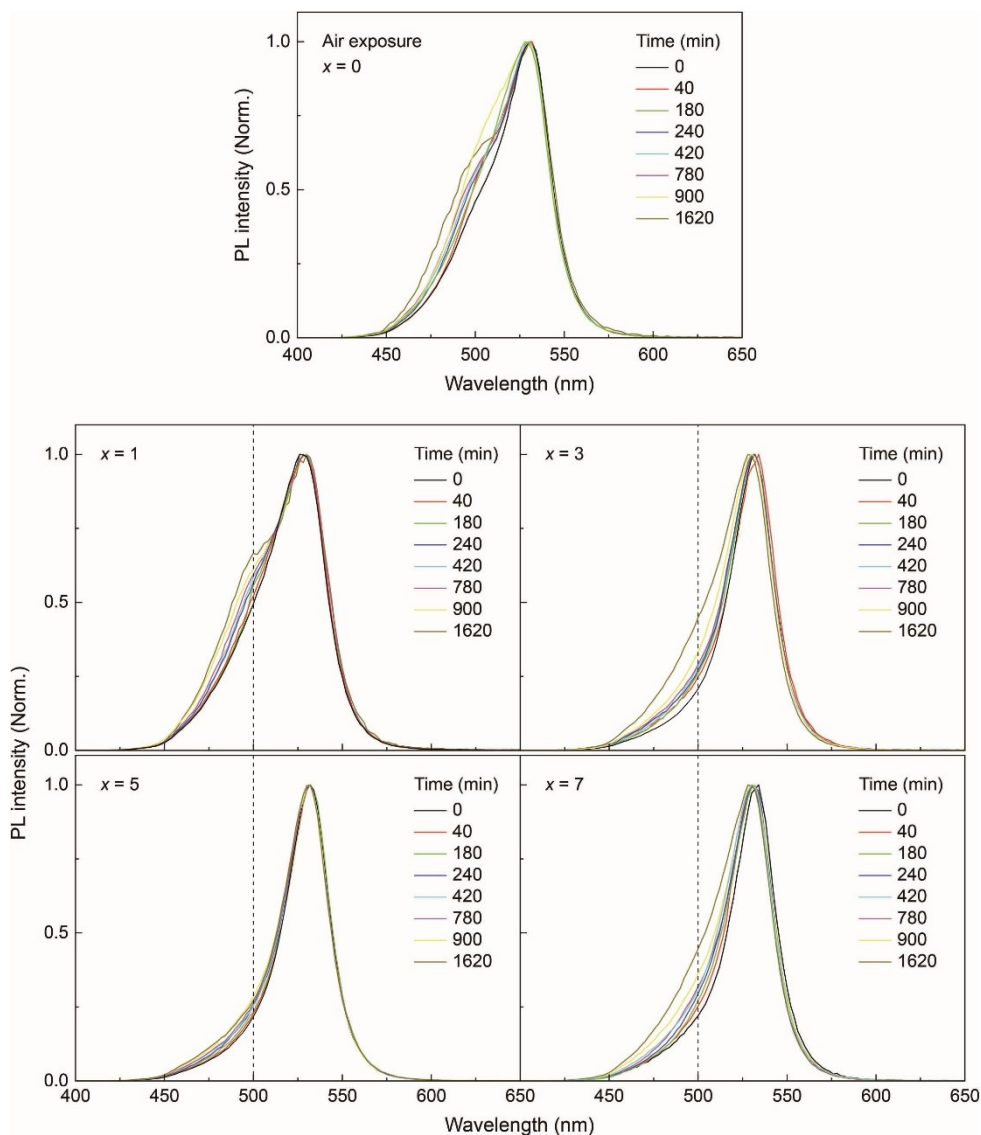


Figure S9. Variations of PL spectra for $x\%$ TPPO:FAPbBr₃ films exposed in air condition for 0-1620 minutes.

When exposed in air, PL spectra of neat FAPbBr₃ film immediately became broadened, due to largely increased emission shoulder peaks in the range of 430-500 nm. A small amount of TPPO additive with $x \leq 1$ has no effect on air stability improvement. In contrast, at $x = 3-7$, PL spectra of the films became much more stable with limited increases of full-width at half-maximum values. Especially, at $x = 5$, PL spectrum of the film was nearly unchanged after air exposure for one day.

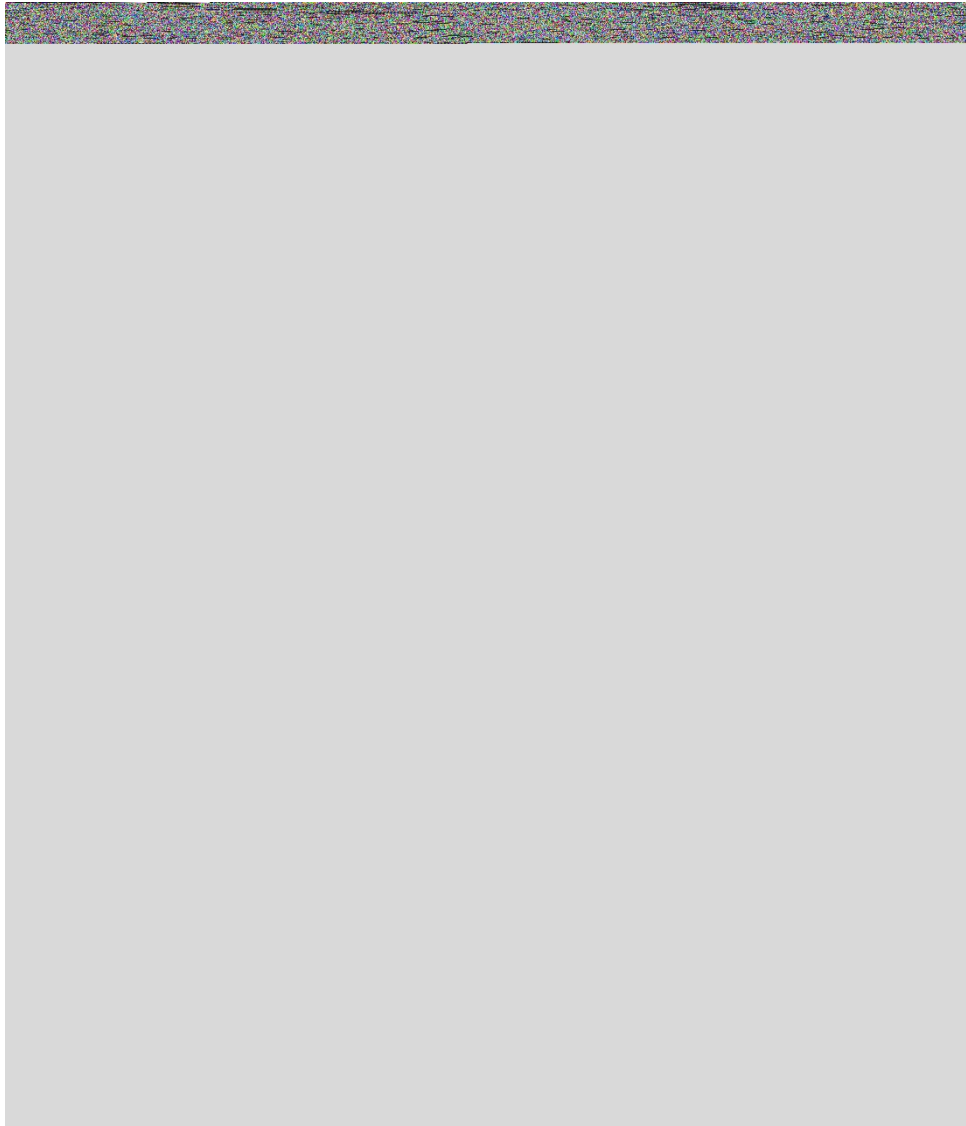


Figure S10. Variations of PL spectra for $x\%$ TPPO:FAPbBr₃ films exposed under 365 UV irradiation for 0-1620 minutes.

Under 365 nm UV light irradiation, PL spectra of neat and 1% TPPO doped FAPbBr₃ films kept unchanged within 40 minutes, but then gradually became broadened, again due to largely increased emission shoulder peaks in the range of 430-500 nm. On the contrary, at $x = 3-7$, PL spectra of the films were basically stable, which did not show obvious changes in the peak wavelengths and profiles. Especially, at $x = 5$, the variation of PL spectrum was negligible despite under UV light irradiation for 1 day.

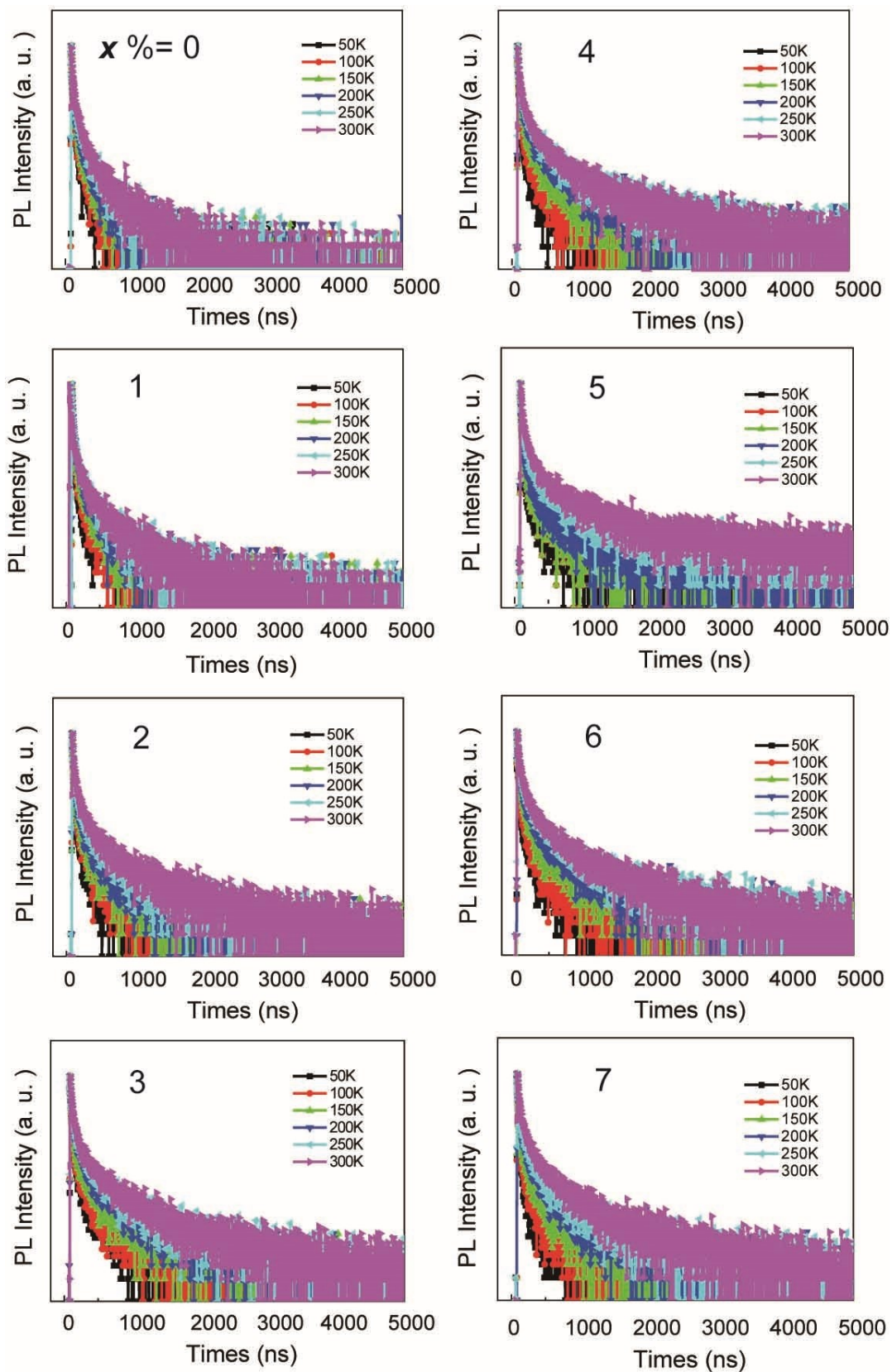


Fig. S11. Time-decay curves of $x\%$ TPPO:FAPbBr₃ films ($x = 0-7$) at temperature range of 50-300 K with an interval of 50 K.